J Mater Sci (2020) 55:3022–3033

Materials for life sciences

The suitability of Synbone® as a tissue analogue in ballistic impacts

Bailey J. Henwood[1,*] and Gareth Appleby-Thomas[1]

[1] *Centre for Defence Engineering, Cranfield Defence and Security, Cranfield University, Defence Academy of The United Kingdom, Shrivenham, Swindon SN6 8LA, UK*

Received: 20 August 2019
Accepted: 7 November 2019
Published online: 22 November 2019

ABSTRACT

Knowledge of material behaviour under impact is of key importance to understand ballistic impact events on tissue. Bone—with its complex underlying microstructure—is no exception; the microstructural network in bone is not only crucial to its integrity, but also provides a pathway for energy dispersion upon impact (Piekarski in J Appl Phys 41:215–225, 1970). Synbone®, a Swiss-made polyurethane bone simulant, has been considered as a potential bone analogue, particularly for cranial structures (Smith et al. in Leg Med 17(5):427–435, 2015; Riva et al. in Forensic Sci Int 294: 150–159, 2019). This study focused on long bone models and cylinders available from Synbone®, with the aim of determining their efficacy for use in ballistic testing and recreation. Comparisons were made between porcine bone and multiple Synbone® models regarding projectile energy loss and damaged surface area using high-speed video and high-resolution photography. CT and reverse ballistics techniques were also used as diagnostic tools. A significant correlation was made between real bone and Synbone®'s ballistic cylinders in all aspects of this study; however, it was observed that osteoporotic cylinders and anatomical models differ significantly in their reaction to impact. Consequently, the use of Synbone® as a ballistic target simulant—particularly when legal or practical accuracy is essential—will need to be treated carefully, giving due attention to these limitations.

Introduction

In ballistic testing and event recreation, understanding the effect of an impact on a material is of particular importance. In high-energy impact situations where a load is applied rapidly, as in ballistic impacts, bone tissue tends to act as a stiff, brittle material, failing instantly [1]. This is in contrast to soft bulk tissues—suggesting that in recreating an event, considerations need to be given to both elements. To this end, a suitable analogue for use in ballistic trauma recreations should have a comparable method of energy dispersion and crack propagation, despite inherent differences in microstructure.

Address correspondence to E-mail: baileyhenwood@gmail.com

https://doi.org/10.1007/s10853-019-04231-y

With any material, the failure mechanism relies heavily on the macrostructure as well as the microstructure. The overall structure of a bone is dependent on the purpose the bone is intended for. There are two fundamental structural configurations: trabecular and cortical [2]. Trabecular bone is generally found in the epiphyses along force planes for stress dampening. These areas are highly porous and lightweight. Cortical bone is denser in comparison, with a very organized microstructure for stability and rigidity in the shaft, or diaphyses, with long bones. The microstructure of both types of bone is composed of Haversian canals, Volkmann canals and various other structures that are used for nutrient and blood transfer. Individual matrix components surrounding the canals are known as lamellae, with the entirety of the nutrient structures and the lamellae being an osteon. Cement lines surround individual osteons and are often the path of least resistance to fractures at low loading rates [3]. Fatigue fractures often occur along cement lines in long bones over time.

Entry wounds from a projectile in human bone can have very distinctive features that can lead investigators to the type of projectile, the distance between the victim and the firearm and the angle of impact. These characteristics are identifiable due to the fracture mode of the bone itself. Bevelling in the bone can differentiate the entry wound from the exit wound, therefore indicating directionality and potentially the angle of impact. Other indicators also noted during entry wound assessment of true bone tissue include cortical flaking and delamination [4]. Calibre estimation may also be conducted using entry wounds; however, the literature on this topic is mostly confined to cranial bones [5–7], with only relatively few studies focussing on long bones [8, 9]. Each of these studies, regardless of the type of bone used, found that a very broad estimate towards calibre can be made. Additionally, information on the type of ammunition may be ascertainable from specific features in an entry wound. Lead rounds classically leave a lead wipe around smooth margins, and the entry wounds are often slightly larger than the calibre of the round. In jacketed rounds, the margins of the entry wound are jagged and appear "chiseled" [9]. The reaction of the bone tissue to different types of ammunition is likely a consequence of the microstructure, and consequently, an analogue may not be able to replicate this exact reaction, making entry wound comparisons more difficult.

In terms of damage modes, during ballistic and other high-energy impacts to long bone, previous studies have indicated that the incident energy is projected through the entire structure without regard for the microstructure [10]. The energy "explodes" into the medullary cavity, where the marrow—under high pressure and strain-rate loading—reacts as a fluid [11]. A permanent cavity results from the projectiles' immediate flight path through the soft tissue; the projectile shears the tissue and it cannot return to an undamaged state. In addition, the resulting temporary cavity can be devastating and is often the most damaging component of a gunshot wound. This transient phenomenon is the response of the soft tissue to the shockwave produced by the projectile during flight through the body. It displaces nerves and blood vessels violently and then falls back into place [11].

One common difficulty in ballistic trauma research is the desire to replicate an injury without facing the ethical and legal complications presented when using human cadaveric tissue. Smith et al. [12] state that cadavers can be difficult to obtain and have the potential to carry infectious risks. However, these issues can be mitigated using alternate materials. Another complication in the use of human tissues is the dynamic nature of a shooting incident. It is not necessarily the case that two gunshot wounds to the same area of the body will result in the same damage. There are many factors to consider, such as age, weight, projectile type, projectile velocity and the distance from the firearm to the victim [12]. In experimental conditions, these factors can all be accounted for, but the heterogenous nature of tissues cannot. The properties of layers of skin, fatty tissue and muscle differ not only between people, but also within an individual—both with location on the body and with age. This leads towards the need for alternative and more consistent options for such ballistic studies.

To reduce the effect of heterogenous tissues during research, synthetic analogues have been proposed and developed from materials such as polyurethane. Such standardized models are designed to alleviate the effect of layers of tissues with differing properties and allow simple bulk tissue analysis to be conducted [11]. In previous research, soft tissue analogues such as ballistic gel and soaps have been validated and are often used in such studies. When conducting research using these analogues, parameters such as

gel thickness, addition of clothing, projectile type, impact velocity and distance may all be altered, and the results can be anticipated [11]. Usefully, analogues also allow easier replication and larger sample sizes, whereas research on real tissues may be restricted to smaller sample sizes. Synthetic samples are often a more readily available option, which are often more morphologically consistent. In addition to the aforementioned benefit of research applications, analogues would also be beneficial in the training of trauma surgeons, or in forensic cases where decomposition or loss of tissue makes analysis difficult.

Synbone® is a Swiss company who began by designing bone models for surgical training and education [13]. Synbone® products are made from polyurethane consisting of isocyanate and polyol and are formed into different models with varying consistency in microstructure. The size and distribution of pores depend on the amount of CO_2 generated during the production of the product using water, silicon and other additives [14]. While originally designed for use in medicine, the Swiss Defence Sector requested models for use in ballistic trauma testing and event recreation. To meet this need, Synbone® has designed their generic models to react the same as bone under ballistic impact [13]. To this end, researchers have been working to ensure that Synbone® is an appropriate analogue for human bone under such circumstances. Outside of the ballistic models, Synbone® has also created cylindrical forms to replicate osteoporotic bone, which is more porous and maybe similar to trabecular bone. Interestingly, the anatomically accurate models are composite layers of differing porosity, much more closely resembling the anatomy of a human long bone than the simpler Synbone® constructs.

In one study, Smith et al. [12] noted that when subjected to ballistic trauma, Synbone® exhibits similar entry wound features to that of natural bone, but that the exit wounds are considerably different. It was therefore strongly suggested that the models should not be used as a method to reliably replicate failure on the microscopic scale in ballistic trauma studies [12]. These differences may be accounted for simply due to the structural difference between the materials [15], underpinning the challenge in deploying an accurate analogue.

The core goal of the work presented in this paper is to continue to both quantify and qualify the reaction of Synbone® products under ballistic impact to determine the suitability for its use as an analogue for bone tissue. To quantify the reaction, both the kinetic energy lost by the projectile during penetration and the damaged surface area of the Synbone® will be calculated and compared to the response of porcine bone impacted in otherwise identical conditions. These measurements are to be calculated from high-speed videos and photographs, respectively. Qualitatively, general crack propagation and fracture patterns will be compared between each type of Synbone® and porcine bone. These features will be observed through photographs, as well as general inspection of the samples. Additionally, reverse ballistics used as a technique that allows diagnostics, such as flash X-ray, to be employed to investigate the interaction of a projectile with respective targets will be used in this study for the same purpose. This technique will be employed in this study for the same purpose. As mentioned, Synbone® only features the generic cylinder and plates in their models for ballistic testing, and therefore, this paper will test those materials as well as osteoporotic samples and anatomical models. It is anticipated that the conclusions drawn may assist in future studies regarding Synbone® as a bone tissue analogue.

Materials and methods

Projectiles

Two types of projectiles, stainless steel and lead, were used for the classic forward ballistic shots. The steel ball bearings had a diameter of 8.0 mm and weighed 2.10 g. The lead balls were 8.4 mm in diameter and weighed 3.47 g. Two projectile materials were chosen to investigate any differences in failure mechanisms due to the impact of yielding versus non-yielding projectiles. The steel ball bearings are meant to simulate those projectiles with metal jackets that do not deform upon impact with bone, while the lead balls are designed to simulate a soft-cored ball round projectile that deforms upon impact.

During the reverse ballistic shots, two bullet types were used: an L2A2 NATO lead ball round and an L2A2 lead ball round with the jacket partially off, exposing the lead core. These rounds were stationary during these tests and, however, will still be referred to as “projectiles” for the sake of clarity.

Targets

Several different types of Synbone® were selected as targets in the forward ballistic investigation, each with differing shapes and/or microstructure. Each piece of Synbone® used was cut to a length of 10 cm.

- A generic cylinder was used to simulate the shaft of long bones, which is the densest of the models selected, at 0.644 g cm^{-3}, measured using an immersion scale and deionized water. This generic cylinder is the model that is intended for use in ballistic testing. The total diameter of the cylinders was 25 mm, with a hollow canal of 9 mm diameter.
- An "osteoporotic" rod was used to simulate the trabecular bone found in the diaphysis of long bones and was extremely porous, with a relative density of 0.172 g cm^{-3}. This was also measured using an immersion scale and deionized water. These rods also have a total diameter of 25 mm, with no hollow canal.
- Finally, anatomical humeri and femora models were also used as targets to determine whether there is a need to use an anatomically correct model when testing ballistic impact damage. These models are produced with two layers; the outer layer is dense to simulate the cortical bone layer, while the inner layer is more porous to simulate the trabecular bone. Both layers differ from the cylinder and the osteoporotic bone in microstructure, therefore not allowing a direct density comparison. The diameter of the humeral shaft was 22 mm, while the diameter of the head was 47 mm. The femur had a shaft diameter of 24 mm with an internal canal of 9.5 mm and a head diameter of 48 mm.

Cross section of samples of each of the four types of Synbone® employed was mounted in resin to observe the microstructure and is shown in Fig. 1. Each sample was captured at 50× magnification.

As a comparison to human bone, porcine humeral bone was selected as a first approximation. The bones were grossly dissected, with very little soft or connective tissues attached. Each bone was cut in half, providing two sections each possessing a shaft portion and a diaphysis. This allowed for some samples to be impacted at the shaft in comparison with the cylinders, while the others could be impacted at the head to compare to the Synbone® anatomical models. The density of porcine bone is approximately 2.1 g cm^{-3} [16].

A 10%, 4 °C ballistic gel was made to simulate the musculature and soft tissue of the human body. Half of the samples of each type of target (Synbone® and bone) were encased in gel, while the other half were left without a soft tissue simulant to identify potential differences in the resultant failure mechanism or energy loss and dispersion.

The mobile targets in the reverse ballistic shots were a portion of 6-mm-thick Synbone® plate fixed to a sabot. Behind the Synbone® plate was a small void to ease visualization of the Synbone® as compared to the sabot on the X-rays. The entire mobile targets—the sabot and the Synbone® together—weighed approximately 286 g.

Shooting

The "Extremely Low Velocity Impact System", or ELVIS, is a 22-mm-bore 1.5-m-long smooth barrelled gun powered by the rapid release of compressed helium gas and was used to fire both the steel and the lead projectiles in the forward ballistics shots. In all cases, projectiles were encased in appropriate 22-mm-diameter sabots on which with the sabot stripped immediately before impact. An impact velocity of approximately 357 ms^{-1} was used for each shot to mimic handgun velocities; requiring 30 bars of helium pressure for the steel projectiles and 34 bars for the lead projectiles. The targets were positioned so the projectiles would impact directly in the centre of the sample, confirmed by an optical laser. Each target was approximately 17 cm away from the muzzle of the gas gun, as shown in Fig. 2.

The reverse ballistics shots were conducted using a 6 m, 50-mm-bore helium-powered gas gun. The helium pressure required to reach a velocity of 750 ms^{-1} was 150 bar. There were four X-ray projections taken at 34 kV to visualize the potential deformation of the projectile and the reaction of the plate's surface upon impact. The distance between the muzzle of the gas gun and the stationary projectile was 80 mm, and the X-rays were timed to be taken 100, 103, 106 and 109 μs after firing. This allowed the four X-rays to capture the progressive penetration of the Synbone® plate by the stationary round of ammunition. A schematic for the set-up of a reverse ballistic investigation is shown in Fig. 3. The

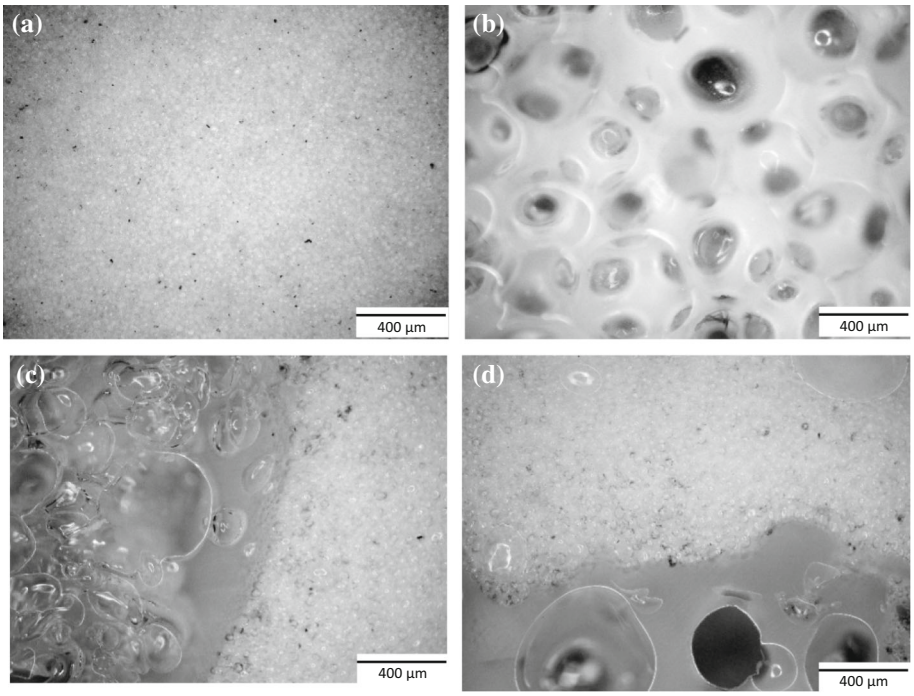

Figure 1 Light microscopy images of four types of Synbone®. **a** Generic cylinder, **b** osteoporotic cylinder, **c** humerus model, **d** femur model.

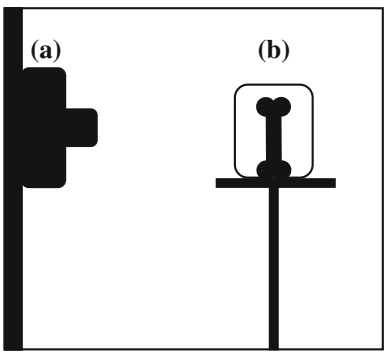

Figure 2 A schematic of the target set-up inside the chamber of ELVIS for all forward ballistics shots.

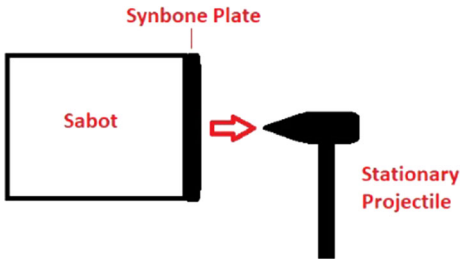

Figure 3 A schematic of the set-up for a reverse ballistic experiment showing the direction of travel for the Synbone® "target", and the stationary round of ammunition.

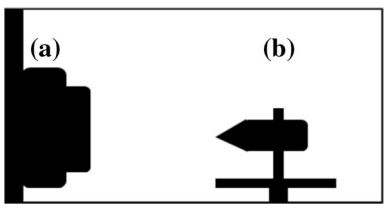

Figure 4 A schematic of the internal configuration for reverse ballistics, where the projectile is held stationary and the Synbone® targets impact the projectile. **a** Muzzle of the gas gun where the sabot and projectile emerge, **b** stationary ammunition (surrounded by X-ray plates).

actual internal configuration of the gun is shown in Fig. 4.

Sample assessment and statistical analysis

High-speed video analysis of each forward ballistic impact was captured and analysed to ascertain the pre- and post-impact velocities of the projectiles, allowing calculation of the respective kinetic energy lost in each target category. In each case, the speed (v) of the bullet was measured within the Phantom® high-speed video program before impacting the target and again upon exit. The kinetic energy was then calculated using $Ke = 0.5\,mv^2$ where the mass (m) was that of the projectile. To negate potential differences in the initial velocity and normalize the data, the percentage of energy lost was calculated

and used in the statistical analysis. The settings for the high-speed videos were as follows: 512 × 352 pixels (resolution), 40,000 frames per second and 5 μs exposure.

High-resolution photographs were taken and used to calculate the surface area of damage sustained at both the entrance and exit sites using the software package ImageJ®. The scale in the photographs was used to calibrate the number of pixels per inch, and the area was selected based on the most external margins of damage sustained by the projectiles. The area of damage sustained by the different Synbone® types was then compared statistically to the porcine bone to determine whether there is consistency in this element of the response between the two materials.

Select samples from each target category were also analysed using computed tomography (CT) to better visualize crack propagation through the polyurethane compared to the porcine bone. These scans further allowed for an overall structural analysis, including pore density and consistency observations. The settings for each scan were as follows: 500 ms exposure time, 85 kV, 65 μA and 2 frames per projection. TIFF stacks were created in 0.1 mm slice in three directions to obtain a complete view of the microstructure: top to bottom, right to left and front to back.

To conduct the statistical analysis for the energy loss of the projectiles, as well as the damaged surface area, IBM SPSS Statistics [17] was utilized to run Levene's test for equal variances, analysis of variance (ANOVA) tests and Dunnett's T3 post hoc test [18].

Results

Projectile energy loss upon impact

The percentage of kinetic energy lost by the projectiles in each Synbone® target subset was calculated and compared to that of the projectiles impacting porcine bone. In each case, the values were checked for normality and equal variances using Levene's statistical test. An analysis of variance (ANOVA) was conducted at $\alpha = 0.05$, and it was found that there was at least one Synbone® target that was comparable in the result. Dunnett's T3 post hoc test was used to determine which of the Synbone® targets supplied the same amount of energy loss to the projectile upon impact as the porcine targets. Table 1 lists those targets that did statistically match the porcine bone.

Damaged surface area

The damaged surface area was measured for each type of Synbone®, as well as the porcine samples, using ImageJ® and high-resolution photographs. Within each type of Synbone®, those subjected to the same conditions—projectile type and the presence or absence of gel—were compared against each other to ensure consistency. Each of the subsets of targets responded with a consistent amount of surface area damage. When these subsets were compared against the porcine samples—again given the same target configurations and projectiles—only one occurrence of consistent area of surface damage was noted. When the generic cylinders with no gel present were impacted with a lead projectile, the area of damaged material was the same as that found in porcine bone with the same conditions ($\alpha = 0.05$, $\rho = 0.0441$). In all other cases, there were no Synbone® materials that sustained the same amount of damage given any target configuration or projectile type. It was notable in the anatomical models that the dense outer layer sustained more damage than the inner layer in terms of measured area. Each of the models showed the inner layer damage being closer to the size of the projectile, whereas the outer layer seemed to be more effected by the energy dispersion laterally, as shown in Fig. 5.

Fracture analysis

Qualitative observations were made on each of the four Synbone® models, in addition to the porcine

Table 1 Significance level of each comparison between the kinetic energy loss by each projectile upon impact with Synbone® targets to that of porcine bone where there was a significant correlation

Projectile	Target material	*P* value (Dunnett's T3)
Lead	Plain cylinder	0.934
	Plain osteoporotic	0.067
	Plain femur	0.055
	Gel cylinder	0.615
	Gel osteoporotic	0.217
Steel	Plain cylinder	0.069
	Gel cylinder	0.699
	Gel osteoporotic	0.565
	Gel humerus	0.094

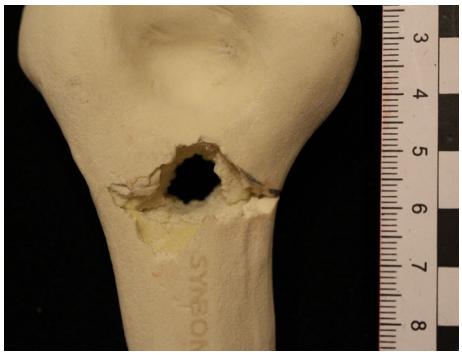

Figure 5 An anatomical humerus model showing the differing reactions between the inner and outer layers.

bone, to compare the propagation of fractures through each material. Because each of the Synbone® types had different densities and pore sizes, the expectation that each would fail differently was met.

All porcine targets, regardless of projectile type or the presence of gel, resulted in round entry wounds with multiple radiating primary fractures. All of the primary fracture lines completely penetrated the bone and created individual fragments. There were also many cases where secondary fractures also occurred and resulted in additional fragments. The fractures that radiated vertically ended at the cut edge of the bone, while the lateral fractures terminated at the exit wound. Figure 6 shows a porcine target that was embedded in ballistic gel and impacted with a lead sphere. In this case, the radiating fractures and their interactions created multiple fragments.

In the generic cylinder samples, when impacted with steel projectiles and regardless of the presence of the ballistic gel, each case showed a depressed ring within the circular entry wound. This phenomenon is shown in Fig. 7. When the generic cylinders were impacted with a lead projectile, there were no samples that had the depressed ring as noted in the steel-impacted samples.

CT was also employed to observe the fracture patterns created in the different types of Synbone®. In Fig. 8, a scan of the generic Synbone® cylinder is compared to the porcine bone. The target configurations were the same; both embedded in gel and impacted with a lead projectile. The red arrows indicate a change in fracture direction where the fracture reaches a change in pore density. It is also notable that compared to the similar case where an embedding ballistic gel cylinder was present (Fig. 7), more extensive impact damage has resulted, likely due to increase in flexure. This clearly highlights the effects of supporting media/bulk tissues and their influence on bone failure.

All of the osteoporotic samples appeared to fail in the same pattern, regardless of the projectile type or the presence/absence of ballistic gel. Each sample was broken into only two fragments by two primary fracture lines on either side of the impact location. In addition, the shape of the entry wound was almond shaped: widest in the centre and tapered to each side, as shown in Fig. 9.

The Synbone® humerus and femur samples fractured in a similar manner to one another given the same projectile type; however, differences were seen when different projectiles were used. Two examples are shown in Fig. 10.

Figure 6 A porcine target impacted with a lead sphere.

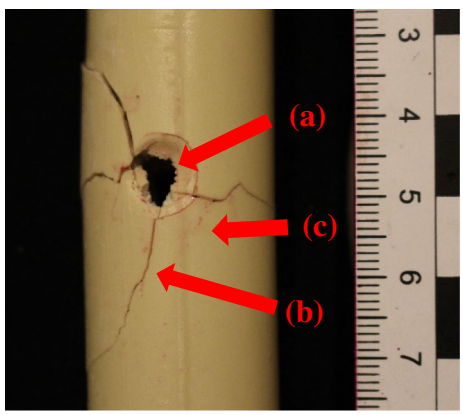

Figure 7 A generic cylinder target: embedded in ballistic gel and impacted with a steel ball. (a) The depressed ring; (b) a primary fracture; and (c) a secondary fracture.

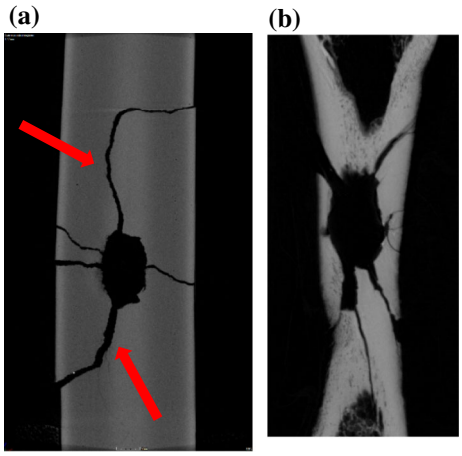

Figure 8 A comparison CT scan of the **a** generic cylinder and **b** porcine bone to observe the fracture patterns and pore structure.

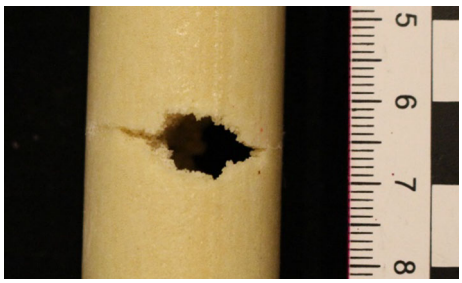

Figure 9 An osteoporotic sample that was embedded in ballistic gel and impacted with a lead ball.

The exit wounds in all Synbone® samples show external bevelling, regardless of the projectile type of the presence of ballistic gel, as shown in Fig. 11. These exit features are more similar to true bone in the anatomical models than the ballistic cylinders.

Reverse ballistics

As the jacketed projectile moved through the Synbone®, there was a conical region ahead of the nose where the pores collapsed before the round made physical contact, as shown in Fig. 12a. The X-rays of the impact using the lead-exposed round show flattening of the nose of the projectile, with no discernable reaction at the surface of the material, differing from the reaction of the material to the jacketed round. Figure 12b shows this region and the deformation of the nose of the lead projectile.

Discussion

Projectile kinetic energy loss

As noted, the generic cylinder had a significant correlation in each target configuration; regardless of the projectile type or the presence of gel, the cylinder supplied the same amount of resistance to the projectile as the porcine bone did. This result supports claims by Synbone® that the generic cylinder may be used in ballistic impact testing in at least one quantitative measure. The osteoporotic Synbone® also produced significant results in three of four configurations. While these targets had a lower significance value than the generic cylinder in all cases, they were still significant, and this result should not be discounted. Further, it was interesting to note that several of these cases involved the presence of ballistics gel—arguably more representative of a real-world tissue arrangement. The anatomical models generally did not produce overall significant results; however, in two cases, there were significant correlations. These target configurations had completely opposing properties; a plain femur impacted by lead and a humerus in gel impacted by steel. While it was recognised that there was the potential for velocity/strain-rate-dependent effects or that the differences in conditions may represent a random correlation, it is interesting that a positive result can be obtained using models designed for surgical use—suggestive

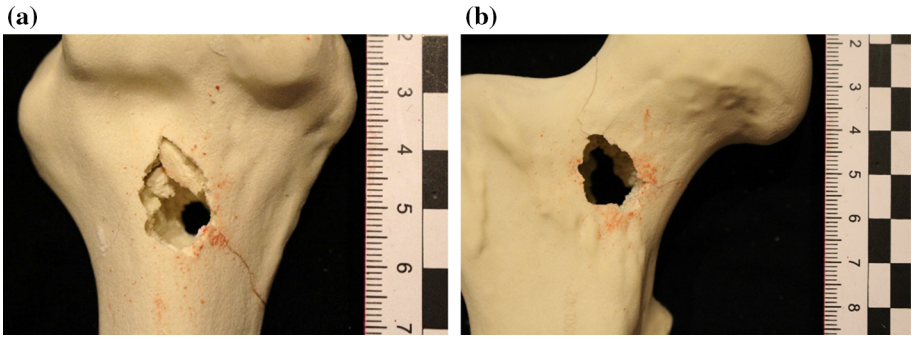

Figure 10 **a** An anatomical humerus impacted with a steel projectile, **b** an anatomical femur impacted by a lead projectile.

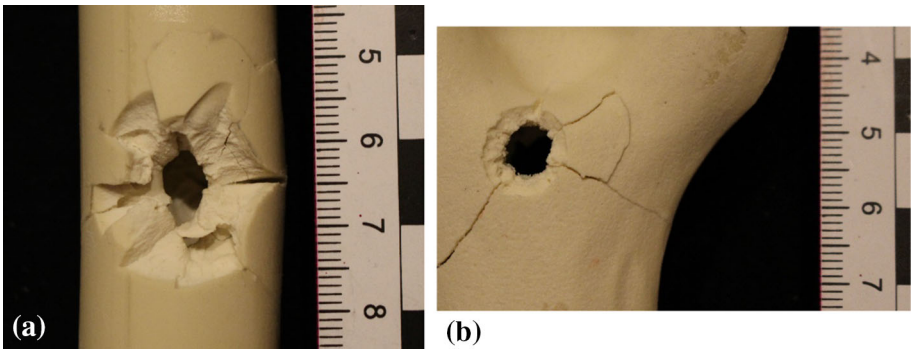

Figure 11 Exit site of two lead projectiles in **a** Synbone® cylinder, **b** Synbone® humerus model, each showing external bevelling.

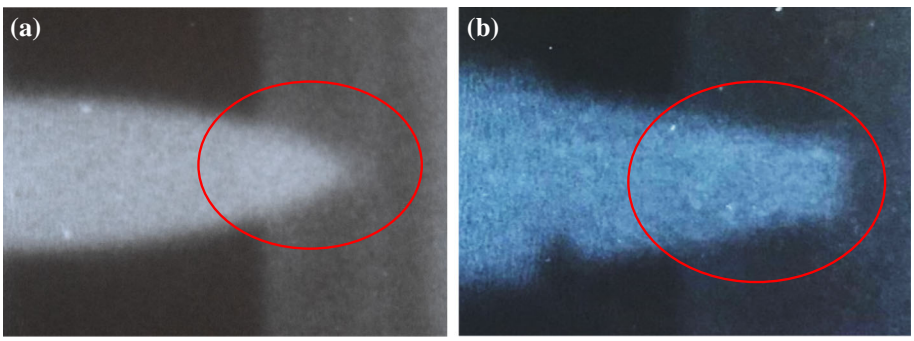

Figure 12 X-rays of the reverse ballistic targets, each identifying the conical region of compressed pores. **a** The non-yielding jacketed projectile entering the Synbone®, **b** the flattened nose of the lead projectile.

that these configurations may be useful from a ballistics standpoint.

Damaged surface area

As previously mentioned, only one case showed the same amount of surface area damage quantitatively. Macroscopically and by visual assessment, the differences between the amount of damage may be attributed to the curvature of the osteoporotic and anatomical models, as they are more rounded than the porcine bone shafts. Another potential explanation for this lack of consistency is simply that the random nature of the microstructure of the models produces unique reactions between the layers within individual samples. Additionally, because each of the impact surfaces was rounded to some extent, ImageJ® cannot account for the curvature, potentially and likely influencing the area calculation—despite of the consistency in the way the photographs were taken, calibrated and analysed.

Fracture analysis

It was noted that in most cases of the Synbone® cylinder, more than two primary fracture lines radiated from the initial entry wound with all terminating at the exit wound. These primary fractures were smooth when ballistic gel was present, and more jagged without gel, indicative of a more ductile response. There were also small surface fractures that did not penetrate the entire cylinder and therefore created fewer fragments. In many cases, a spontaneous change in fracture direction was noted. This behaviour was originally thought to have been due to a random large pore; however, there are no obvious voids that would cause this phenomenon. In both CT scans conducted on ballistic cylinders, there is at least one instance of a fracture changing direction at the margin between the two regions of differing pore densities. This must be reviewed carefully; as within the same samples, other fracture lines show no regard for the change in pore density. There is potential that the change in pore density designed into the cylinders affects the fracture propagation; however, not enough samples were scanned to draw any conclusions. The porcine sample does not exhibit fractures that suddenly change direction, therefore allowing the assumption that the polyurethane pore-based microstructure provides an alternate failure mechanism.

In general terms, the cylinder behaved more like the actual bone tissue than the other Synbone® models, as expected. Generally, each cylinder did display comminuted fractures, with at least two

primary fractures producing multiple fragments. This does not in itself allow for a seamless comparison; however, there are some broad generalizations that can be made towards the similarities. On a very general scale, these cylinders could be utilized in ballistic impact studies; however, it is not recommended that conclusions be made regarding fragment sizes or crack propagation patterns. Interestingly, the presence or absence of a depressed ring in the generic cylinders may indicate a possibility in terms of determining the type of ammunition used; this was also noted in one study where the steel ammunition left a noticeably different entry wound to the lead ammunition [9]. While this study did not find the *same* differences, there may be some indication that the type of ammunition may be ascertainable in the Synbone® cylinders as well. There was no cortical bending or delamination noted, also mentioned by other literature on this topic [4]. No measurements were made for calibre estimation; however, the sizes of the entry wound could be a further area for study.

When observing the osteoporotic samples, the wound channel appeared to be completely pulverized by both type of projectile, where the pore margins have been broken by the passing projectile. Each sample broke into two pieces by two primary fracture lines which spanned from the entry to exit points. There were no depressed rings in any case, nor was any bevelling noted. These samples did not exhibit any similarities to the porcine bone.

Anatomical samples impacted with a steel projectile at the epiphysis remained in one piece without any complete fractures. There were, however, some small pieces of the dense outer layer broken off and lodged into the entry wound, as shown in Fig. 11a. In the few targets where radiating fractures did occur, they terminated 1–3.5 cm from the entry wound and did not result in any fragments. In cases where the shaft was impacted, all samples fractured into two fragments due to two radiating fractures originating at the entry wound and terminating at the exit wound. For those samples surrounded by gel, the radiating fractures were smoother than those without the gel layer; however, the dense outer layer was more damaged surrounding the entry wound. In turn, the anatomical models impacted with lead projectiles at the epiphysis again remained intact, while the shaft samples fractured into two fragments. The difference seen in the lead-impacted samples was primarily the sharpness of the entry wound edges and the lack of fragments lodged into the entry wound.

When concerned with the exit wounds in the Synbone® samples, external bevelling was noted and is a feature often utilized as a diagnostic for identifying gunshot wounds in real-life cases [4]. Bevelling was seen in the exit wounds of the cylinder samples as well as the anatomical humeri and femora models and, however, was more similar to true bone in the anatomical models. The bevelling in the cylinders is more exaggerated and stepped than in the anatomical models or real bone, as shown in Fig. 12. This supports that while specific comparisons between the reaction of Synbone® to ballistic impact are not entirely possible, the bevelling features can be used to indicate an area of damage as the exit point of the projectile and differentiate it from an entry point.

Reverse ballistics

A major benefit to using reverse ballistics is that projectiles that naturally yaw inside of targets are held stable and level [14, 19]. This allows for the visualization of the interaction between the projectile and the target material. In the interest of identifying failure mechanism differences given yielding and non-yielding projectiles, two L2A2 NATO ball rounds were used: one as manufactured with the copper jacket intact and one where the jacket had been removed, exposing the lead core.

As the jacketed projectile moved through the Synbone®, there was a conical region ahead of the nose where the pores collapsed before the round makes physical contact, as shown in Fig. 12a. The assumption can made that the shockwave ahead of the projectile is causing pore collapse in the material. No deformation of the projectile was noted, and there appeared to be a very slight outward buckle of the material immediately adjacent to the entry point of the projectile. When the lead projectile was used, while there was still a region of pores that collapsed ahead of the projectile, it was a narrower cone than the previous result. While faint, this area is still visible on the X-ray films.

From the results of both reverse ballistics trials, it is apparent that Synbone® undergoes pore collapse ahead of the projectile's nose due to the leading shockwave generated on projectile impact. While the general pore collapse region is conical in both

yielding and non-yielding situations, showing a successive, cascading collapse of pores ahead of the projectile, the size of that cone varies between the two conditions. While these tests were conducted with flat plates of Synbone®, the microstructure and density are similar to that of the generic cylinder, and the results may therefore also allow insight into the failure of the cylinders. It may be interesting to also see how bone tissue reacts as an additional level of comparison in future studies.

Limitations and future work

The main limitation of this study is the sample size of each target category. Due to cost and time restraints, only three shots per target configuration were performed, each reconstructed and photographed for analysis. These restraints also limited the amount of CT scans that could be conducted. If there had been more cylinder samples scanned, a more thorough investigation could have been made into the sudden change in direction at the pore density change margins. Secondly, when calculating both the speed of the projectile and the damaged area, subjective measurements were used. To mitigate this effect in both cases, the high-speed videos and photographs were assessed twice, each on different dates. It is postulated that this would hopefully minimize human error and allow for average values to be used. Thirdly, because ImageJ® cannot recognize a curved surface, the area calculations were made using 2D images of 3D objects. This methodology comes with an inherent caveat; however, the parameters for area selection were kept consistent, hopefully minimizing the effect.

In future studies, the use of real ammunition in the classic forward ballistics portion of such work may prove useful. For example, the lack of spin imparted on the projectiles may alter the fracture mechanism and associated propagation through the target materials. Additionally, using real ammunition would change the force density at the leading edge of the projectile. The ball bearings used in this study have a greater impact surface than a true round of ammunition, which may again alter crack propagation and directionality. Finally, while the scope of this study did not include a direct assessment of the microstructural reaction to a ballistic impact, it would be of value to investigate to further support the use of Synbone® as a bone tissue analogue.

Conclusions

A series of ballistic impact experiments were conducted on Synbone® products to ascertain their suitability as a bone tissue analogue. Both classic forward ballistic and reverse ballistic impact tests were conducted to investigate projectile energy loss upon impact, surface area of damage and the assessment of failure mechanism and crack propagation through the materials. The findings of this study support the use of Synbone®'s generic cylinder in ballistic impact studies to some extent;

1. In all cases, the energy lost by a projectile impacting a generic cylinder is the same as when the same projectile impacts porcine bone. This was not generally true for that of the osteoporotic or anatomical models; however, some similar results were noted.
2. The overall fracture patterns of the Synbone® models were not entirely similar to the porcine bones; however, very broad generalizations could be made, such as the complete comminution of the cylinders and porcine bone. Consequently, it is apparent that these models should not be relied upon for entry wound feature analysis or crack propagation replication and estimation.
3. Exit "wounds" in the Synbone® models show external bevelling, allowing the differentiation from a projectile's entry point. This is a similar reaction as that of true bone, however, not entirely visually comparable.
4. Finally, the failure of the polyurethane pore structure occurs before physical contact with the ammunition and appears to be due to the leading shockwave. A Hertzian-like conical area of damage is noted in most samples as the pores compress and ultimately collapse. This is dissimilar to bone tissues.

Overall, Synbone®'s models may be a suitable analogue for bone tissues, barring the caveat that visual inspection of the entry wounds in any of their models is not completely like true bone tissue. A purely quantitative design may be more appropriate for future studies using Synbone® as a bone tissue analogue.

Acknowledgements

The work contained in this paper was completed within a Master of Science in Forensic Ballistics at Cranfield University by the primary author. The authors would like to express the deepest gratitude to Andy Roberts and Dave Miller for their work with the targets and gas guns, Fiona Brock for her work with the computed tomography and Christine Grey without whom this project would not have come to fruition and also to Rachael Hazael and John Rickman for their insight and support.

Compliance with ethical standards

Conflict of interest The authors have no conflict of interest to declare.

Electronic supplementary material: The online version of this article (https://doi.org/10.1007/s10853-019-04231-y) contains supplementary material, which is available to authorized users.

References

[1] Berryman H, Lanfear A, Shriley N (2012) The biomechanics of gunshot trauma to bone: research considerations within the present judicial climate. In: Dirkmaat D (ed) A companion to forensic anthropology. Blackwell Publishing Ltd, West Sussex, pp 390–399

[2] Rho J, Kuhn-Spearing L, Zioupos P (1998) Mechanical properties and the hierarchal structure of bone. Mech Eng Phys 20:92–102

[3] Piekarski K (1970) Fracture of bone. J Appl Phys 41:215–225

[4] DiMaio V (2016) Gunshot wounds; practical aspects of firearms, ballistics and forensic techniques, 3rd edn. CRC Press, Boca Raton

[5] Berryman H, Smith O, Symes S (2007) Diameter of cranial gunshot wounds as a function of bullet calibre. J Forensic Sci 52(3):751–754

[6] Ross A (1996) Calibre estimation from cranial entrance defect measurements. J Forensic Sci 41:629–633

[7] Paschall A, Ross A (2017) Bone mineral density and wounding capacity of handguns; implications for estimation of caliber. Int J Leg Med 45:161–166

[8] Berryman H, Gunther W (2000) Keyhole defect production in tubular bone. J Forensic Sci 45(2):123–131

[9] Henwood B, Oost T, Fairgrieve S (2019) Bullet caliber and type categorization from gunshot wounds in *Sus scrofa* (Linnaeus) long bone. J Forensic Sci. https://doi.org/10.1111/1556-4029.14004

[10] Cohen H, Kugel C, May H, Medlej B, Stein D, Slon V, Hershkovitz I, Brosh T (2016) The impact velocity and bone fracture pattern. Forensic Perspect 266:54–62

[11] Kneubuehl B, Coupland R, Rothschild M, Thali M (2008) Wound ballistics. Springer, Berlin

[12] Smith M, James S, Pover T, Ball N, Barnetson V, Foster B, Guy C, Rickman J, Walton V (2015) Fantastic plastic? Experimental evaluation of polyurethane bone substitutes as proxies for human bone in trauma simulations. Leg Med 17(5):427–435

[13] Synbone® (2019) Portfolio for ballistic testing. https://www.synbone.com/app/uploads/2017/01/1484314977-b61bc01138a7d03c233f8e8eec59462c.pdf. Accessed 13 Apr 2019

[14] Fitzmaurice B (2014) On the properties and suitability of Synbone as a tissue simulant. M.Sc. dissertation, Cranfield University

[15] Riva F, Lombardo P, Zech W, Jackowski C, Schyma C (2019) Individual synthetic head models in wound ballistics-a feasibility study based on real cases. Forensic Sci Int 294:150–159

[16] Aerssens J, Boonen S, Lowet G, Dequeker J (1998) Interspecies differences in bone composition, density and quality: potential implications for in vivo bone research. Endocrinology 139(2):663–670

[17] IBM SPSS Statistics for Windows (2015) version 23.0.0.2

[18] Everett B, Shrondal A (2010) The Cambridge dictionary of statistics, vol 4. Cambridge University, Cambridge

[19] Appleby-Thomas GJ, Jaansalu K, Hameed A, Painter J, Shackel J, Rowley J (2019) A comparison of ballistic behaviour of conventionally sintered and additively manufactured alumina. Def Technol. https://doi.org/10.1016/j.dt.2019.06.020